

Conduction delays can enhance formation of up and down states in spiking neuronal networksPavel M. Esir,^{1,2,*} Susan Yu. Gordleeva,² Alexander Yu. Simonov,^{1,2} Alexander N. Pisarchik,³ and Victor B. Kazantsev²¹*Department of Theory of Oscillations and Automatic Control, N. I. Lobachevsky State University of Nizhny Novgorod, 603050 Nizhny Novgorod, Russia*²*Department of Neurotechnology, N. I. Lobachevsky State University of Nizhny Novgorod, 603050 Nizhny Novgorod, Russia*³*Center for Biomedical Technology, Technical University of Madrid, Madrid, 28223, Spain*

(Received 30 October 2017; revised manuscript received 17 September 2018; published 1 November 2018)

We study dynamics of a spiking network of synaptically connected bistable neuronal oscillators. We find that delays in axonal conduction result in the emergence of coexisting states with high and low activity levels (up and down states). In the network, where cellular bistability is present, propagation delays and noise play a crucial role in the emergence of transitions between the states.

DOI: [10.1103/PhysRevE.98.052401](https://doi.org/10.1103/PhysRevE.98.052401)**I. INTRODUCTION**

The spontaneous transition between up and down states characterized by high and low firing rates in cortex and striatum is a well-known phenomenon [1–3]. Many theoretical models have been developed to explain the dynamics of this kind of transition [4–8]. This phenomenon still continues to attract the attention of theoreticians [9–11].

Typically, transitions from up to down states cannot be achieved without inhibition. The inhibitory population stabilizes a self-sustained up state by preventing the system from over-excitation [7,12,13]. If inhibition is not present, the continuously growing excitation can be prevented by a short-term depression [6].

In stochastic models, noise induces switches between stable attractors in the network. However, apart from stochastic transitions, there is also another mechanism of switching between up and down states. In the up state, a slow potassium current deactivates the system and switches it to the down state. After a while, the network restores its activity and switches again to the up state [5].

In addition to these known scenarios, in the present work we suggest a mechanism for the appearance of up and down states. We show that up and down states can emerge even without any inhibition, short-term depression, or slow inactivating currents. The key factors in our model, apart from noise, are axonal conduction delays and cellular bistability.

Networks consisting of type-I excitable neurons, whose dynamics can be described by a leaky integrate-and-fire model, in some circumstances allow mean-field approximation and were studied in detail [11,14,15]. The influence of delays on neural dynamics was studied previously [16–22]. For example, in a simple rate model it was shown that delays can significantly enrich the repertoire of dynamical regimes in neuronal networks [16]. In addition, the delays in neuronal networks can lead to the appearance of so-called polychronous groups [17]. It should be noted that delayed dynamical systems

with single-unit bistability and simple potential wells were extensively studied in many papers [18–20]. Moreover, it was also shown that increasing delays leads to the same effect as increasing the synaptic current decay constant; namely, it stabilizes self-sustained persistent activity [11]. However, to the best of our knowledge, the mechanism of transitions between up and down states appearing from the influence of delays in networks of type-II excitability excitatory neurons was not previously considered.

The second important feature of our model is single-neuron bistability. Cellular bistability in neurons was previously reported in many theoretical and experimental works [23–26], as well as bistability at the network level [6,27–31]. Since noise is always present in real neuronal networks [32], its influence on the network dynamics is of great importance, especially in the presence of multistability [33,34]. In multistable systems, noise often leads to multistate intermittency [35,36]. In many cases, noise plays a constructive role resulting in well-known phenomena, such as stochastic and coherence resonances, found in the standard Hodgkin-Huxley neuron model [37,38] and in neuronal networks [39]. Interestingly, two bistable neurons subjected to noise can exhibit synchronous episodic discharges [28]. In a large noisy network, bistability can contribute to stabilization of neuron clusters [29,40,41].

In this paper, we develop a mathematical model to describe the formation of up and down states. Our model includes the following key factors: conduction delays, cellular bistability, and noise. In contrast to previous studies, our model is free from inhibitory neurons, short-term plasticity, and slow inactivation currents.

II. MODEL

Let us consider a recurrent network of synaptically coupled bistable Hodgkin-Huxley (HH) neurons [42]. The membrane potential of a single neuron evolves according to the following ionic current balance equation:

$$C \frac{dV^{(i)}}{dt} = I_{\text{channel}}^{(i)} + I_{\text{app}}^{(i)} + \sum I_{\text{syn}}^{(ij)} + I_P^{(i)}, \quad (1)$$

*esir.pavel@gmail.com

where the superscripts (i) and (j) denote the indices of post- and presynaptic neurons, respectively. Ionic currents (e.g., sodium, potassium, and leak currents) are expressed as follows:

$$I_{\text{channel}} = -g_{Na}m^3h(V - E_{Na}) - g_Kn^4(V - E_K) - g_{\text{leak}}(V - E_{\text{leak}}),$$

$$\frac{dx}{dt} = \alpha_x(1 - x) - \beta_x x, \quad x = m, n, h, \quad (2)$$

where α_x and β_x are nonlinear functions for gating variables taken as the ones in the original HH model with the exception that the membrane and reversal potentials are shifted by 65 mV. Throughout this paper, we use the following parameter values: $E_{Na} = 55$ mV, $E_K = -77$ mV, $E_{\text{leak}} = -54.5$ mV, $g_{Na} = 120$ mS/cm², $g_K = 36$ mS/cm², $g_{\text{leak}} = 0.3$ mS/cm², and $C = 1$ μ F/cm². The applied currents $I_{\text{app}}^{(i)}$ are fixed to control the depolarization level and dynamical regimes, which can be excitable, oscillatory, or bistable [28,43]. The synaptic current I_{syn} simulating interactions between neurons obeys the following equations:

$$\frac{dI_{\text{syn}}}{dt} = c - \frac{I_{\text{syn}}}{\tau_{\text{syn}}},$$

$$\frac{dc}{dt} = -\frac{c}{\tau_{\text{syn}}} + \frac{w_{\text{syn}}e}{\tau_{\text{syn}}}\delta(t - t_{sp} - d), \quad (3)$$

where $\tau_{\text{syn}} = 0.2$ ms is the synaptic time, w_{syn} is the synaptic weight (in μ A/cm²), the normalizing coefficient e is the Euler number, c is a synaptic variable (in μ A/ms cm²), w_{syn} is the peak value of the excitatory postsynaptic current (EPSC), δ is the Dirac delta function, t_{sp} is the presynaptic spike timing, namely, the time when the membrane potential reaches its peak value (~ 25 mV), and d is the conduction delay. Upon arriving at the presynaptic terminal, the spike evokes EPSC with the peak amplitude w_{syn} at the postsynaptic neuron in the form of an α function given as

$$I_{\text{syn}}(t) = w_{\text{syn}} \left(\frac{t - t_{sp} - d}{\tau_{\text{syn}}} \right)_+ \left(e^{-\frac{t - t_{sp} - d}{\tau_{\text{syn}}}} \right)_+, \quad (4)$$

where $(x)_+ = \max(0, x)$ are Macaulay brackets to cut off negative values.

Each neuron is stimulated by a Poisson pulse train mimicking external spiking inputs $I_p^{(i)}$ of a certain rate λ . Similar to inter-neuron communication, each Poisson spike evokes a response in the form of the α function refined by Eq. (4), but with amplitude w_p .

First, let us consider the dynamics of a single neuron. The applied current $I_{\text{app}}^{(i)}$ controls neural excitability, i.e., its dynamical mode, which can be excitable, oscillatory, or bistable. The neuron in the excitable mode exhibits a single stable steady state. If an external perturbation exceeds a threshold value, the neuron responds with a short excitation pulse (spike) and returns back to the stable steady state. In the oscillatory mode, the neuron generates a periodic spike sequence forming a stable limit cycle, being the only attractor in the phase space. In the parameter region between excitable and oscillatory modes, Hodgkin-Huxley neurons are known to exhibit bistability [23,28]. In this region, a stable fixed point coexists with a limit cycle and their basins of attraction are

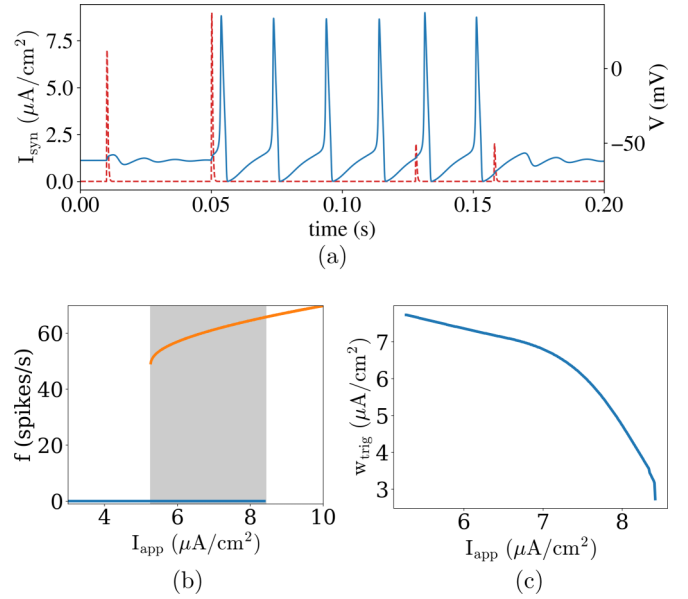


FIG. 1. (a) Membrane potential (solid blue line) and synaptic current (dashed red line) of the bistable neuron response to several incoming spikes for $I_{\text{app}} = 5.27$ μ A/cm². (b) Spiking frequency as a function of depolarizing current. The bistability area is shaded. (c) Minimal weight required for switching the bistable neuron from quiescent to active state as a function of depolarizing current.

separated by an unstable manifold. Transitions between these two coexisting states can be triggered by a sufficiently strong external stimulus.

Figure 1(a) shows the response of a single neuron to several incoming spikes of different strengths. Depending on its weight and phase, a spike can evoke subthreshold excitatory postsynaptic potential (EPSP), switch the neuron to an oscillatory state of regular spiking, or switch the neuron from the oscillatory to the steady state. The spiking frequency depends on the applied current as shown in Fig. 1(b), where the bistability area is shaded. For the set of parameters used in this paper, bistability appears at $I_{\text{app}} = [5.270, 8.416]$ μ A/cm².

One can see from Fig. 1(c) that the minimal threshold weight w_{trig} of a single incoming spike required for turning the neuron to the oscillatory state decreases as applied current I_{app} is increased. This can be qualitatively explained in the following way. A pair of limit cycles appears when the system in Eq. (1) undergoes a fold limit cycle bifurcation. Near the border of the excitable mode, the state separating manifold is closer to the stable limit cycle, and the attraction domain of the stable steady state is much larger than that of the stable limit cycle. Therefore, the smaller the external current I_{app} , the greater the weights of the external events required for turning the neuron to the active state, and the easier to turn the neuron back to the silent state. In the latter case, in addition to the weight it is also important to consider a relative phase of the stimulus application time [28,44].

Let us now construct a network of spiking neurons described by Eq. (1). We assume that each of $N = 100$ neurons operates in the bistable mode ($I_{\text{app}} = 5.27$ μ A/cm²). We also assume that the action potentials propagate with a constant velocity. Then, we calculate the values of the conduction

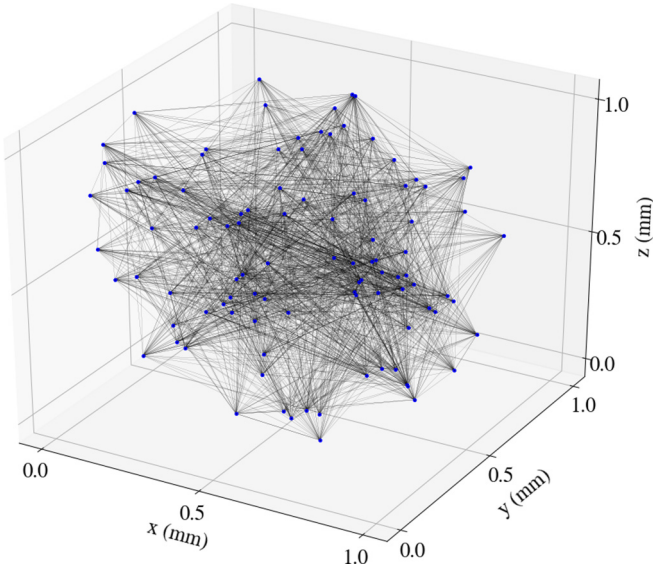


FIG. 2. Schematic view of the network topology. All neurons are located in a cubic volume of a 1-mm side.

delays as $d_{ij} = s_{ij}/V_{ap}$, where s_{ij} is the physical distance between the neurons and $V_{ap} = 0.05$ m/s is the velocity of action potential propagation. The resulting delays hit the physiological range 0–20 ms [45,46]. In geometrical space, the neuron’s position is chosen randomly within a cubic volume shown in Fig. 2. The connection probability for each pair of neurons is fixed to $p_{con} = 0.2$.

III. RESULTS

A. Synchronization and time-locked clusters of activity

Let us now consider spiking dynamics of the neuronal network without delays ($d = 0$) and without any noise ($I_p^{(i)} = 0$). As expected [47], in this case the system demonstrates

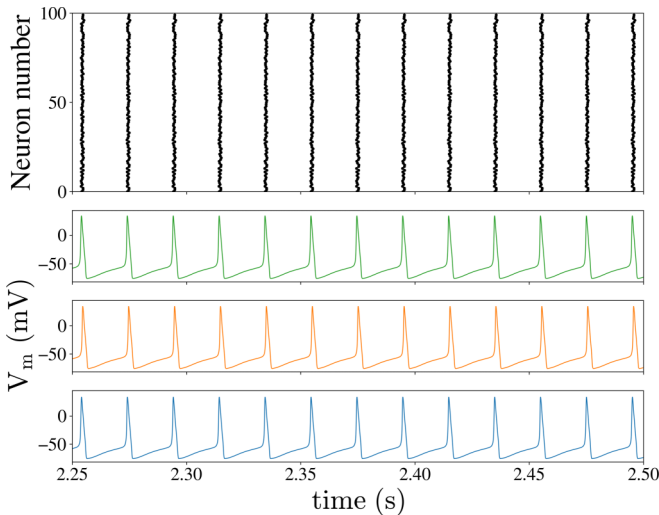


FIG. 3. Synchronization in the neuronal network without delays and without external input for $w_{syn} = 1.3 \mu\text{A}/\text{cm}^2$. Bottom: Membrane potentials of three randomly chosen neurons with indices 9, 40, and 92.

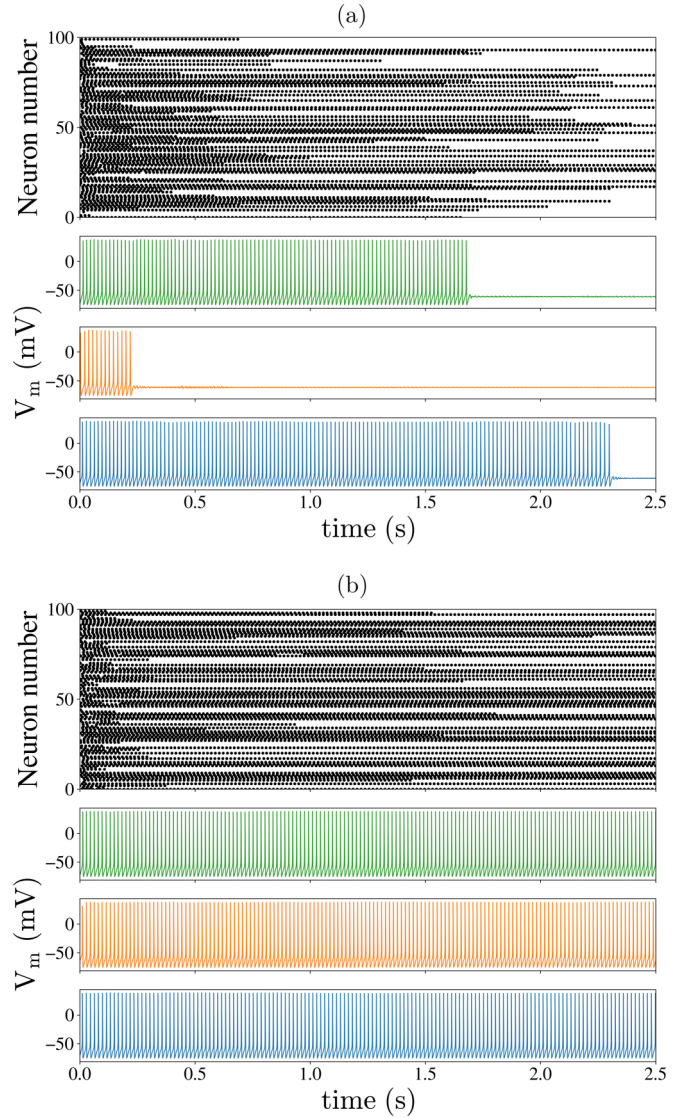


FIG. 4. Formation of time-locked patterns in the presence of delays. Simulations in (a) and (b) have different initial conditions.

synchronous dynamics with a spiking frequency close to the values of the isolated neuron (as seen from Fig. 3). In the figure, the upper panel shows a raster plot of the network activity, where each dot represents a spike. The examples of membrane potential traces of three randomly chosen neurons are shown in three subsequent graphs below the raster.

After including conduction delays, the network dynamics dramatically changes. Depending on the initial conditions, the network exhibits distinct stable activity patterns, where only a part of the neurons oscillate (Fig. 4). The figures illustrate highly multistable network dynamics. Such time-locked patterns have millisecond precision, as illustrated in Fig. 5.

Note that without coupling delays, different time-locked patterns disappear and the network activity converges either to synchronous oscillations or to an equilibrium state.

To examine the stability of the time-locked patterns, we add small noise to the network ($w_p < 0.5 \mu\text{A}/\text{cm}^2$). Due to the robustness of the patterns to noise, this small

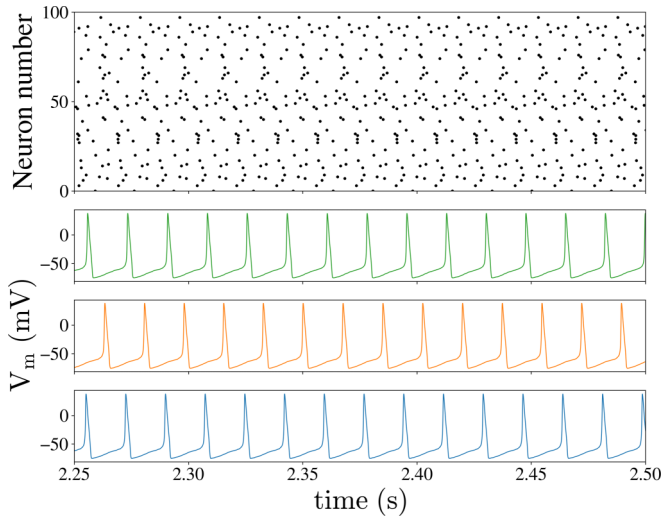


FIG. 5. Time-locked patterns from Fig. 4(b) when the network is fed by weak noise $w_p = 0.4 \mu\text{A}/\text{cm}^2$. Noise is turned on starting from 2.5 s.

perturbation of the membrane potential does not destroy the neural dynamics, so that all observed spiking patterns preserve their shapes (see Fig. 5). However, higher intensity noise destroys the time-locked patterns [Fig. 6(a)]. Note that the probability to knock out a single neuron to an equilibrium state is higher than in the case of $w_p \simeq 0.5$. This leads to a faster noise-induced deactivation of the whole network when w_p is increased [Fig. 6(b)]. For smaller noise, the duration of the deactivation stage increases and tends to infinity for vanishing noise. Because the simulation time is finite, we do not consider here the details of the deactivation process for low noise intensities ($w_p < 0.5 \mu\text{A}/\text{cm}^2$).

B. Up and down states

Let us now stimulate the network by higher intensity noise ($w_p > 1.5 \mu\text{A}/\text{cm}^2$). In this case, noise can turn a single neuron from equilibrium to an oscillatory state. Interestingly, in this case the network dynamics exhibits only two specific dynamical modes of asynchronous spiking with high and low mean firing rates of the whole network (up and down states), as shown in Figs. 7 and 8.

To illustrate this situation, we take the amplitude of Poisson spikes, w_p , as a control parameter and vary it within a certain range. The right-hand panel in Fig. 8 shows traces of the firing rate for different values of w_p . For each trace, the system starts from initial conditions corresponding to the up state, and after a transient process the dynamics converges to a certain stationary state. In the first case, the network is in the deactivated down state [Fig. 8(a)]. In this state, however, the neurons are not completely silent, exhibiting rare spiking with a relatively low level of firing rate. The rare asynchronous spikes appear due to the Poisson pulse drive. The opposite situation is characterized by the active up state with a relatively high level of firing rate [Fig. 8(e)].

The most interesting case is observed when the network displays spontaneous transitions between the high and the low firing rates, which we call up and down states [Figs. 8(b)–

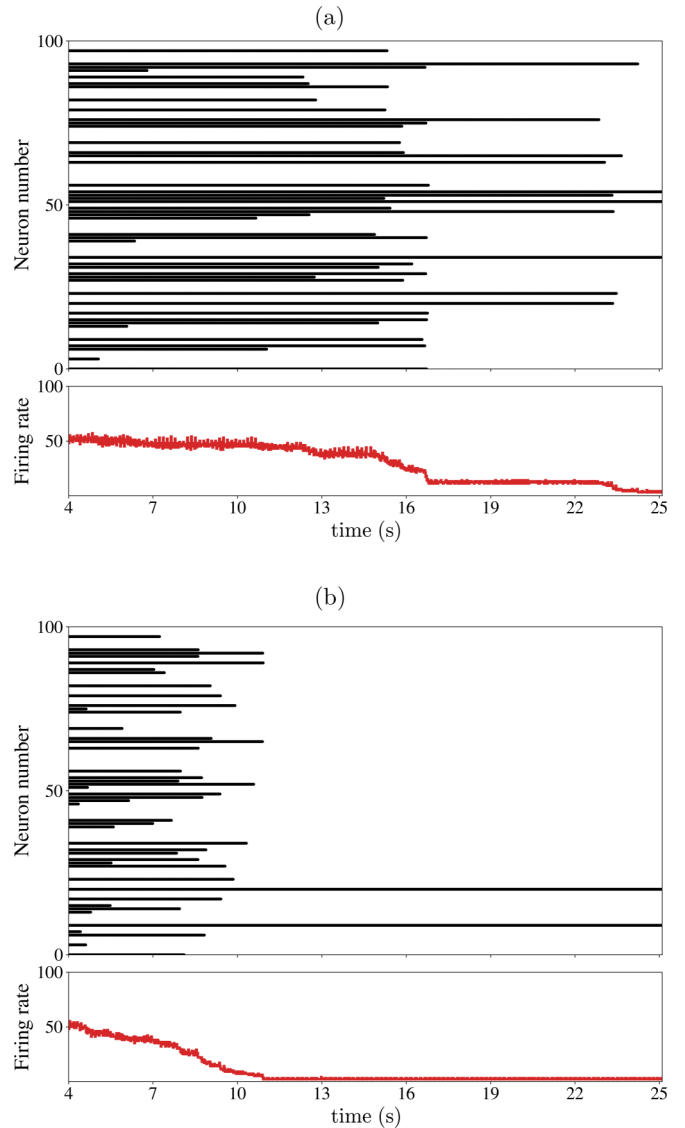


FIG. 6. Network activity in the presence of low noise. The firing rate is estimated as the number of spikes in the 20-ms time window. After a transition process, stable time-locked patterns are formed and noise is turned on at 4 s. (a) $w_p = 0.5 \mu\text{A}/\text{cm}^2$. During the simulation time, the noise knocks out only a part of the neurons. (b) $w_p = 0.7 \mu\text{A}/\text{cm}^2$. After 11 s, the noise knocks almost all neurons to an equilibrium state.

8(d)]. Note that the histograms of firing rate have two apparent peaks [Figs. 8(b)–8(d)]. Depending on the noise level, the network stays during certain time intervals in the neighborhood of up and down states.

The formation of up and down states could be explained as follows. Noise of sufficiently high intensity can induce switches in neuron dynamics from a quiescent steady state to an oscillatory state or vice versa. The activation of a sufficient part of the network can also induce a transition to the up state. This process occurs in an avalanche manner because the more neurons are active, the easier new neurons enter an active phase. Conversely, the deactivation of a sufficient part of the network can induce a transition to the down state. This stochastic process depends on the phases of Poisson

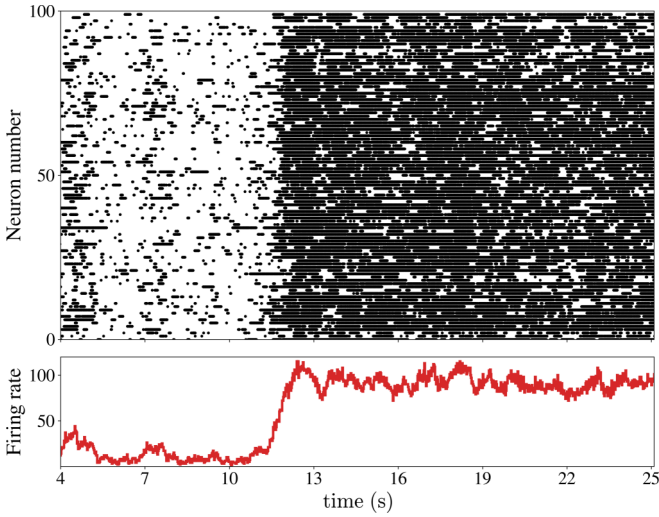


FIG. 7. Network transition to the state with high mean firing rate when Poisson noise is sufficiently strong, $w_p = 1.97 \mu\text{A}/\text{cm}^2$.

noise spikes which affect neurons. Thus, in the presence of sufficiently strong noise, the network states with intermediate firing rates (Fig. 6) become unstable, and the network dynamics becomes bistable with pronounced up and down states (Figs. 7 and 8).

Since in our case all synaptic currents are excitatory, due to cellular bistability an incoming postsynaptic potential with an appropriate phase may switch a single neuron to a quiescent state. Therefore, each time interval, the number of active and inactive neurons may change depending on the time of spikes and axonal conduction delays. This process compensates for the lack of inhibition, short-term depression, and slow inactivating currents. To the best of our knowledge, this mechanism of switches was never examined, though the coexistence of two attractive states was previously observed in

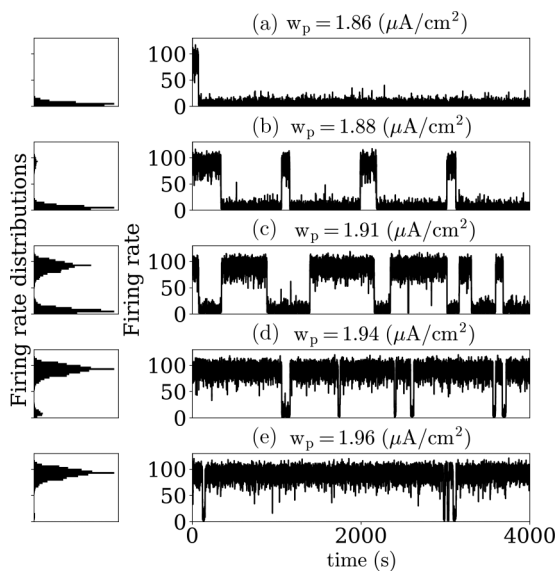


FIG. 8. Examples of population activity driven by noise of different intensities w_p . Firing rate traces (right) and their histograms (left) for $\lambda = 185 \text{ Hz}$ and $w_{\text{syn}} = 1.3 \mu\text{A}/\text{cm}^2$.

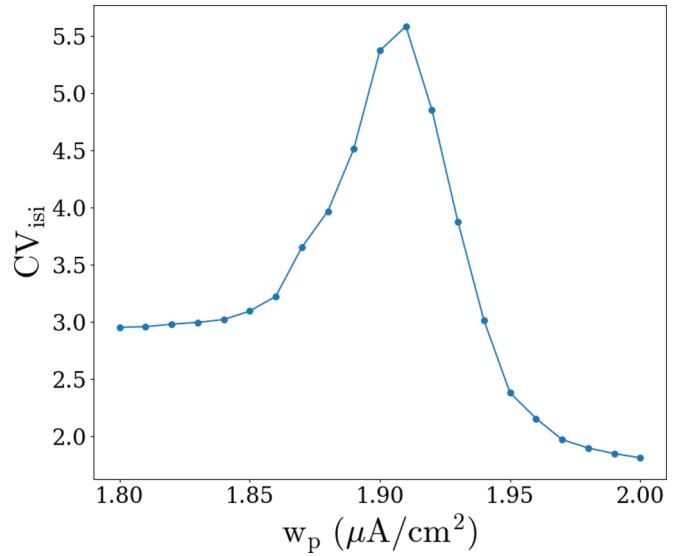


FIG. 9. Dependence of ISI variation on noise amplitude w_p for $\lambda = 185 \text{ Hz}$ and $w_{\text{syn}} = 1.3 \mu\text{A}/\text{cm}^2$. Each point represents the result of 40 simulations with 10^4 s duration.

recurrent networks [48]. Our results demonstrate that spontaneous jumps between up and down states are only possible if type-II excitatory neurons are present in the network without inactivating currents and short-term depression.

The transitions between the up and down states are found in a narrow range of the synaptic weights $w_{\text{syn}} \in [1.8, 2.0]$ for fixed values of other parameters. However, the variation of connection probability p_{con} can shift this range.

C. Statistics of inter-spike intervals

The statistics of inter-spike intervals (ISIs) of neurons in the network is very important for correct interpretation of the obtained results. The ISI variation coefficient was calculated as the standard deviation to the mean ratio. Interestingly, unlike other typical excitable systems stimulated by noise [37–39,49], our model does not exhibit coherence resonance. In our case, the ISI variation coefficient has an apparent maximum with respect to w_p (see Fig. 9). The position of this maximum corresponds to the value of w_p at which the histograms of firing rate distributions (Fig. 8, left) contain two peaks with approximately the same amplitudes. In this case, the system spends approximately the same amount of time in the neighborhood of each metastable state.

D. Multiple time scales of metastable states

To characterize the network metastable dynamics, we also calculate distributions of metastable lifetimes. The threshold for separating intervals of active and quiescent states is 50 spikes/time bin. The time interval distributions in the active state, T_{up} , and in the quiescent state, T_{down} , are plotted in Fig. 10 in logarithmic scale. The distributions are calculated for 1920 simulations, each of which lasted 10^4 s . Interestingly, the time interval distributions exhibit two characteristic time scales. We use power-law and exponential-law approximations for the lower and higher ranges of the time intervals, respectively. The probability density function approximating

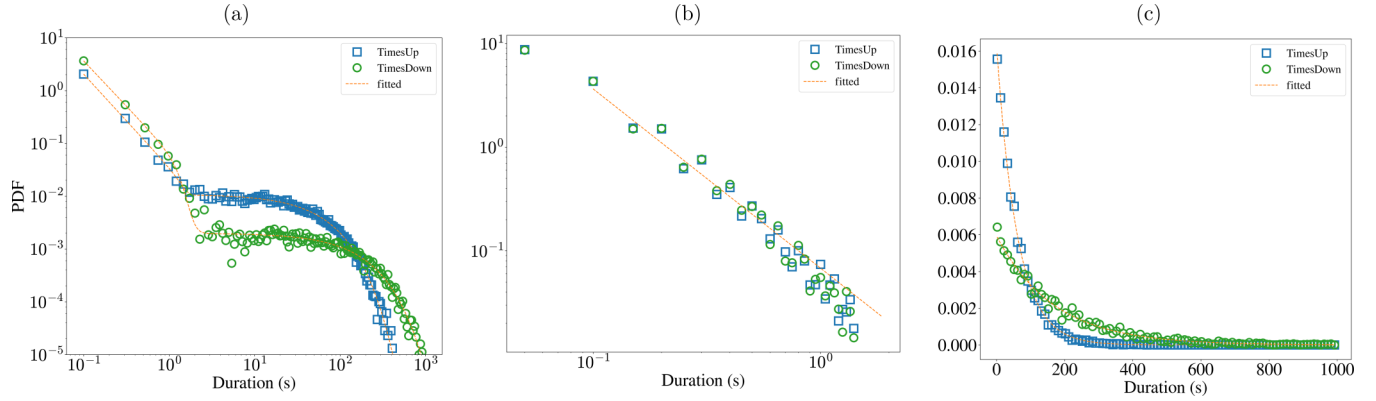


FIG. 10. Distributions of metastable state durations. (a) Exponential distribution for large durations and power law for small durations. (b), (c) Zoomed fragments of the distributions: blue squares, up-state durations; green circles, down states. The parameters of the probability density functions (PDF) approximating our data are the following: for up states, $T_{\text{up}} n_1 = 1.708$, $n_2 = 0.006$, $n_3 = 4.358$, $a_1 = 0.072$, $a_2 = 0.002$, and $b = 1.318$; for down states, $T_{\text{down}} n_1 = 1.708$, $n_2 = 0.006$, $n_3 = 4.360$, $a_1 = 0.072$, $a_2 = 0.002$, and $b = 1.318$. $w_p = 1.91 \mu\text{A}/\text{cm}^2$.

our data has the following form:

$$p(x) = (1 - p_0(x)) \frac{a_1}{x^{n_1}} + p_0(x) a_2 e^{-n_2 x},$$

$$p_0(x) = \frac{1}{1 + e^{-n_3(x-b)}}, \quad (5)$$

where the sigmoidal function p_0 determines the weights of the two distributions and separates them. It is parametrized by the slope n_3 and by the midpoint b . The other parameters are n_1 , the power-law exponent, n_2 , the rate of the exponential distribution, and a_1 and a_2 , the normalization coefficients. We use the least squares method to estimate the parameter values of the weighted sum.

In contrast to the paper of Mejias *et al.* [9], where the authors report a power-law distribution obtained with a rate model under a noisy short-term depression, our results demonstrate both the exponential- and the power-law statistics. The main reason for this probably is that synapses in our case are deterministic and moreover do not exhibit short-term depression. More detailed study of this question may be the subject of a future study.

IV. CONCLUSION

We conclude that up- and down-state dynamics can be generated by a network of spiking bistable neurons with axonal conduction delays. In contrast to previous studies, in our case this effect is observed without any inhibitory neurons, short-term synaptic plasticity, and slow inactivation currents. The key factors that lead to the formation of the up and down states are coupling delays, intrinsic cellular bistability, and noise.

The transitions between up and down states were found within a narrow range of parameters. In our model, the transitions were observed in relatively small networks with a size ranging from 50 to 120 elements. The connection weights were adjusted for different network sizes. When the network size was increased, the durations to stay in the up state also increased, and finally the transitions did not appear during the simulation time, when the network size became larger than

120. Interestingly, the network size is known to be comparable to the size of cortical minicolumns [50].

While switching dynamics of a single bistable neuron from the oscillatory state to the quiescent (Fig. 1) depends on the relative times of incoming spikes [28], network dynamics is determined by connection delays. Our numerical simulations showed that the transitions occurred for the conduction delay values within the following ranges: $d \in [2, 2.75]$, $[3.25, 4.25]$, $[9.25, 10.5]$. More detailed studies of the dependence of neural switching dynamics on the coupling delays can be a subject of further research.

The formation of persistent spike-timing patterns is another interesting result of our work. A particular pattern profile is determined by the connectivity matrix, the delays between neurons, and initial conditions. As known from earlier modeling studies, the delay distribution pattern can encode a number of dynamical states called polychronous groups [17]. These groups are formed by a repeated sequence of spikes transmitted from presynaptic to postsynaptic neurons. The number of such patterns can be enormously large. Being robust to noise, the patterns preserve their configurations if noise is relatively small. However, an increase in the noise intensity leads to the disappearance of states with small basins of attraction, which means that stronger noise simplifies the system. A surprising situation occurs in the case of relatively high noise intensities. For certain noise intensities, the precise timing structure is destroyed and the spike firing becomes asynchronous. We found that within such asynchronous spiking, the whole network firing can be described as the interplay of two states, one with low and another with high average firing rate, i.e., up and down states.

Notably, there is an optimal noise rate when the inter-spike interval variation coefficient has an apparent maximum. In this case, the network resides in the up and down states equally.

In this work, we have analyzed a relatively small set of parameters and regimes due to an extremely high computational cost of the Hodgkin-Huxley model. More comprehensive analysis of larger networks may be a subject of future research using simplified models of type II or models which allow mean-field approximation.

ACKNOWLEDGMENTS

This research was supported by the Russian Science Foundation (Grant No. 16-12-00077) and the Russian Foundation for Basic Research (Grant No. RFBR 16-32-60145).

-
- [1] R. L. Cowan and C. J. Wilson, *J. Neurophysiol.* **71**, 17 (1994).
 [2] M. Steriade, A. Nuñez, and F. Amzica, *J. Neurosci.* **13**, 3266 (1993).
 [3] I. Lampl, I. Reichova, and D. Ferster, *Neuron* **22**, 361 (1999).
 [4] M. V. Sanchez-Vives and D. A. McCormick, *Nat. Neurosci.* **3**, 1027 (2000).
 [5] A. Compte, M. V. Sanchez-Vives, D. A. McCormick, and X.-J. Wang, *J. Neurophysiol.* **89**, 2707 (2003).
 [6] D. Holcman and M. Tsodyks, *PLoS Comput. Biol.* **2**, e23 (2006).
 [7] N. Parga and L. F. Abbott, *Front. Neurosci.* **1**, 57 (2007).
 [8] A. Destexhe, *J. Comput. Neurosci.* **27**, 493 (2009).
 [9] J. F. Mejias, H. J. Kappen, and J. J. Torres, *PLoS One* **5**, e13651 (2010).
 [10] D. Jercog, A. Roxin, P. Barthó, A. Luczak, A. Compte, and J. de la Rocha, *eLife* **6**, 1 (2017).
 [11] E. M. Tartaglia and N. Brunel, *Sci. Rep.* **7**, 1 (2017).
 [12] D. Hansel and G. Mato, *Phys. Rev. Lett.* **86**, 4175 (2001).
 [13] G. Mongillo, D. Hansel, and C. van Vreeswijk, *Phys. Rev. Lett.* **108**, 158101 (2012).
 [14] D. J. Amit and N. Brunel, *Cerebral Cortex* **7**, 237 (1997).
 [15] N. Brunel, *J. Comput. Neurosci.* **8**, 183 (2000).
 [16] A. Roxin, N. Brunel, and D. Hansel, *Phys. Rev. Lett.* **94**, 238103 (2005).
 [17] E. M. Izhikevich, *Neural Comput.* **18**, 245 (2006).
 [18] D. Huber and L. S. Tsimring, *Phys. Rev. Lett.* **91**, 260601 (2003).
 [19] L. S. Tsimring and A. Pikovsky, *Phys. Rev. Lett.* **87**, 250602 (2001).
 [20] D. Huber and L. S. Tsimring, *Phys. Rev. E* **71**, 036150 (2005).
 [21] J. M. Sausedo-Solorio and A. N. Pisarchik, *Phys. Lett. A* **378**, 2108 (2014).
 [22] J. M. Sausedo-Solorio and A. N. Pisarchik, *Eur. Phys. J. Spec. Top.* **226**, 1911 (2017).
 [23] J. Rinzel and R. N. Miller, *Math. Biosci.* **49**, 27 (1980).
 [24] E. M. Izhikevich, *IEEE Trans. Neural Networks* **14**, 1569 (2003).
 [25] G. Huaguang, Z. Zhiguo, J. Bing, and C. Shenggen, *PLoS One* **10**, e0121028 (2015).
 [26] Y. Loewenstein, S. Mahon, P. Chadderton, K. Kitamura, H. Sompolinsky, Y. Yarom, and M. Hausser, *Nat. Neurosci.* **8**, 202 (2005).
 [27] M. A. Komarov, G. V. Osipov, and J. A. K. Suykens, *Chaos* **18**, 037121 (2008).
 [28] V. B. Kazantsev and S. Y. Asatryan, *Phys. Rev. E* **84**, 031913 (2011).
 [29] A. Litwin-Kumar and B. Doiron, *Nat. Neurosci.* **15**, 1498 (2012).
 [30] P. Miller and X. J. Wang, *Chaos* **16**, 026109 (2006).
 [31] X. J. Wang, *J. Neurosci.* **19**, 9587 (1999).
 [32] A. A. Faisal, L. P. Selen, and D. M. Wolpert, *Nat. Rev. Neurosci.* **9**, 292 (2008).
 [33] J. Braun and M. Mattia, *NeuroImage* **52**, 740 (2010).
 [34] A. N. Pisarchik and U. Feudel, *Phys. Rep.* **540**, 167 (2014).
 [35] A. N. Pisarchik, R. Jaimes-Reátegui, R. Sevilla-Escoboza, and G. Huerta-Cuellar, *Phys. Rev. E* **86**, 056219 (2012).
 [36] A. E. Hramov, A. A. Koronovskii, O. I. Moskalenko, M. O. Zhuravlev, R. Jaimes-Reategui, and A. N. Pisarchik, *Phys. Rev. E* **93**, 052218 (2016).
 [37] Y. Wang, D. T. Chik, and Z. D. Wang, *Phys. Rev. E* **61**, 740 (2000).
 [38] S.-G. Lee, A. Neiman, and S. Kim, *Phys. Rev. E* **57**, 3292 (1998).
 [39] A. V. Andreev, V. V. Makarov, A. E. Runnova, A. N. Pisarchik, and A. E. Hramov, *Chaos Solitons Fractals* **106**, 80 (2018).
 [40] W. Wei, F. Wolf, and X. J. Wang, *Phys. Rev. E* **92**, 032726 (2015).
 [41] M. Camperi and X. J. Wang, *J. Comput. Neurosci.* **5**, 383 (1998).
 [42] A. L. Hodgkin and A. F. Huxley, *J. Physiol.* **117**, 500 (1952).
 [43] E. Izhikevich, *Dynamical Systems in Neuroscience: The Geometry of Excitability and Bursting* (MIT Press, Cambridge, MA, 2007).
 [44] A. Y. Simonov, S. Y. Gordileeva, A. N. Pisarchik, and V. B. Kazantsev, *JETP Lett.* **98**, 632 (2014).
 [45] H. A. Swadlow, *J. Neurophysiol.* **54**, 1346 (1985).
 [46] H. A. Swadlow, *J. Neurophysiol.* **71**, 437 (1994).
 [47] S. Boccaletti, A. N. Pisarchik, C. I. del Genio, and A. Amann, *Synchronization: From Coupled Systems to Complex Networks* (Cambridge University Press, New York, 2018).
 [48] S. Fusi and M. Mattia, *Neural Comput.* **11**, 633 (1999).
 [49] A. S. Pikovsky and J. Kurths, *Phys. Rev. Lett.* **78**, 775 (1997).
 [50] V. B. Mountcastle, *Brain* **120**, 701 (1997).